Numerical solutions of Green's integral equation for the diffraction of femtosecond laser pulses through a subwavelength aperture

Xiaorong Ren (任晓荣)[1,2], Chuanfu Cheng (程传福)[1,2], Chunxiang Liu (刘春香)[2], Hongsheng Song (宋洪胜)[2], Ningyu Zhang (张宁玉)[3], and Zhizhan Xu (徐至展)[1]

[1]*Shanghai Institute of Optics and Fine Mechanics, Chinese Academy of Sciences, Shanghai 201800*

[2]*Department of Physics, Shandong Normal University, Ji'nan 250014*

[3]*Shandong Institute of Architecture and Engineering, Ji'nan 250014*

Received September 18, 2003

In this letter, we propose a method for the numerical calculations of the femtosecond laser pulse passed through a subwavelength aperture. The time-dependent laser pulse is decomposed into a series of monochromatic simple harmonic waves. For the light field of the harmonic wave with a single frequency, the numerical calculation is made based on the solution of the Green's integral equation set of the electromagnetic waves. Such numerical solution is iterated for all the waves with different frequencies, and all the numerical solutions are transformed into the light fields in the time domain by inverse Fourier transform. The light intensity distributions transmitted the subwavelength aperture are calculated and the results show the propagation of the light field is along the direction of the medium interface.

OCIS codes: 050.1220, 320.2250, 140.7090.

Near-field optics is a new area which deals with the propagation of light waves within the region of a subwavelength distance from the medium interface[1,2], and it provides the theoretical foundations for the engineering of the scanning near-field optical microscopy[3]. One of the important subjects in near-field optics is the diffraction of light waves through the subwavelength aperture which is directly associated to the fabrication of near-field fiber probes and hence has attracted great attention in the past years[4−9]. It is well understood that laser pulses with ultrashort duration may induce a lot of new physical phenomena in its propagation and its interaction with matter[4−7]. The diffraction of the femtosecond laser pulses through a subwavelength aperture is the combination of the near-field optics and femtosecond spectroscopy and is promising in opening up new fields of studies[6,7].

In the studies of near-field optics, two kinds of numerical methods, i.e., the finite-difference time domain method (FDTD)[8,9] and the rigorous solutions of Green's integral equations[10,11], have been developed. In the present literature, all the time-dependent problems in near-field optics are treated with FDTD. The method of Green's integral is easier and more expediency when the near-field light field problems involve irregular boundaries. In this letter, we extend the Green's function method to solve the subwavelength aperture diffraction of femtosecond laser pulse. We expand the femtosecond laser pulse with Gaussian temporal profile as the sum of a series of harmonic waves. For each of the harmonic waves, the integral equations on the interface are numerically discretized into a linear equation set. The solutions of the linear equation set give the spatial numerical distribution of the wave field. By Fourier-transforming the superposition of the wave field solutions of all the single frequency waves at the same spatial point, the time-dependent wave field at this spatial point is obtained. The results show that the transmitted intensity distributions in the near-field region produced by femtosecond laser pulse through a subwavelength aperture are not symmetric with respect to time any more as the incident femtosecond laser pulse.

Figure 1 shows the diagram for the propagation of the light wave at the medium interface. We discuss the one-dimensional case for simplicity. An s-polarized parallel light wave $E^i(\mathbf{r})$ with a vacuum wavelength λ perpendicular to the coordinate plane $z = 0$ is incident on the interface of the dielectric media, here $\mathbf{r}$ is the position vector. The medium interface is an aperture with length L. To demonstrate the principles of the Green's integral method, we suppose the medium surface has a height distribution $z = D(x)$ in the following theoretical analysis though $D(x)$ may set to be zero for the diffraction through the aperture. In the left half space, $z > D(x)$, the relative dielectric constant of medium $\varepsilon = n_d^2$ is real, and the right half space, $z < D(x)$,

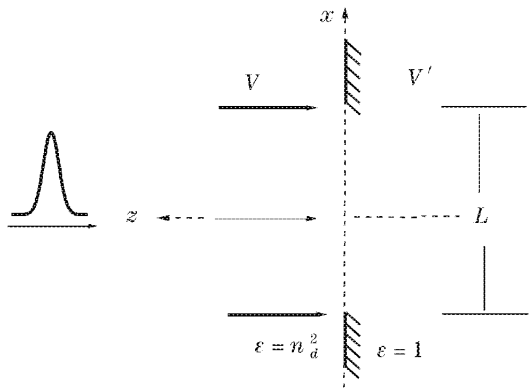

Fig. 1. The diagram for the diffraction of a laser pulse through a subwavelength aperture.

is vacuum. The lateral range of the aperture is $[-L/2, L/2]$. The femtosecond laser pulse can be assumed to be a Gaussian shape in time[5,6]

$$E^{(i)}(\mathbf{r},t) = E_0 \mathrm{e}^{-(\frac{t}{\tau})^2} \mathrm{e}^{i\omega_0 t}, \tag{1}$$

where τ denotes the full width at half-maximum of the pulse and ω_0 denotes the central frequency of the pulse. The time-dependent light wave may be regarded as the superposition of a series of monochromatic components with different frequencies

$$E^{(i)}(\mathbf{r},t) = \int E^{(i)}(\mathbf{r},\omega)\mathrm{e}^{-i\omega t}\mathrm{d}\omega, \tag{2}$$

$E^{(i)}(\mathbf{r},\omega)$ can be simply obtained from the Fourier transform of $E^{(i)}(\mathbf{r},t)$ and the time harmonic form of the light wave of a single frequency is

$$E^{(i)}(\mathbf{r},\omega_i)\mathrm{e}^{-i\omega_i t} = \tau\sqrt{\pi}E_0 \mathrm{e}^{-\frac{\tau^2}{4}(\omega_i-\omega_0)^2}\mathrm{e}^{-i\omega_i t}. \tag{3}$$

The electric fields of the waves $E(\mathbf{r},\omega)$ and $E'(\mathbf{r},\omega)$ in the left half-space V and right half-space V', respectively, satisfy Helmholtz equation[12]

$$\nabla^2 E(\mathbf{r},\omega_i) + k_i^2 E(\mathbf{r},\omega_i) = 0\ , \quad z > D(x),\ (\mathbf{r}\in V)\ , \tag{4a}$$

$$\nabla^2 E'(\mathbf{r},\omega_i) + k_{i0}^2 E'(\mathbf{r},\omega_i) = 0\ , \quad z < D(x),\ (\mathbf{r}\in V')\ , \tag{4b}$$

where $k_{i0} = |\mathbf{k}_{i0}| = \omega_i\sqrt{\mu_0\varepsilon_0}$ and $k_i = \sqrt{\varepsilon}k_{i0}$ are the moduli of the wave vectors and here ε_0 and μ_0 are the vacuum dielectric constant and the magnetic permeability, respectively. In the left space, $E(\mathbf{r},\omega_i)$ is the sum of the incident wave and the scattered wave from the surface. $E(\mathbf{r},\omega_i)$ and $E'(\mathbf{r},\omega_i)$ satisfy the following boundary conditions for the s-polarized waves

$$E(x,\omega_i) = E[x, D(x),\omega_i] = E'[x, D(x),\omega_i], \tag{5a}$$

$$F(x,\omega_i) = \gamma[\frac{\partial E(\mathbf{r},\omega_i)}{\partial n}]_{z=D^{(+)}(x)} = \gamma[\frac{\partial E'(\mathbf{r},\omega_i)}{\partial n}]_{z=D^{(-)}(x)}, \tag{5b}$$

where $E(x,\omega_i)$ and $F(x,\omega_i)$ are the electric field and the its derivative at the interface, respectively. $D^{(+)}$ and $D^{(-)}$ represent, respectively, the surface approaching the interface $D(x)$ from the left and right half-spaces. $\frac{\partial}{\partial n} = (\mathbf{n}\cdot\nabla)$, $\mathbf{n} = (1/\gamma)[D'(x), 1]$, $\gamma = \{1 + [D'(x)]^2\}^{1/2}$, and $D'(x)$ represents the derivative of $D(x)$ with respect to x. Applying the Green's integral theorem to the Helmhotz equations (4a) and (4b) together with the above boundary conditions, the electric fields at the medium surface satisfy the following integral equation set[10]:

$$E(x,\omega_i) = E^{(i)}[x, D(x),\omega_i] + \frac{1}{4\pi}\int_{-\infty}^{+\infty}\mathrm{d}x' \left\{E(x',\omega_i)[\frac{\partial G}{\partial z'} - D'(x')\frac{\partial G}{\partial x'}] - GF(x',\omega_i)\right\}, \tag{6a}$$

$$-\frac{1}{4\pi}\int_{-\infty}^{+\infty}\mathrm{d}x' \left\{E'(x',\omega_i)[\frac{\partial G_0}{\partial z'} - D'(x')\frac{\partial G_0}{\partial x'}] - G_0 F(x',\omega_i)\right\} = 0, \tag{6b}$$

where $G_0 = G_0(x,x',\omega_i)$ and $G = G(x,x',\omega_i)$ are, respectively, the one-dimensional Green's functions in the right and left half-spaces:

$$G_0(\mathbf{r},\mathbf{r}',\omega_i) = i\pi H_0^{(1)}(k_0|\mathbf{r}-\mathbf{r}'|), \tag{7a}$$

$$G(\mathbf{r},\mathbf{r}',\omega_i) = i\pi H_0^{(1)}\left\{[\varepsilon(\omega)]^{1/2}k_0|\mathbf{r}-\mathbf{r}'|\right\}, \tag{7b}$$

with $H_0^{(1)}$ being the zero-order Hankel function of the first kind. Accordingly, the electric field $E'(\mathbf{r},\omega_i)$ in the right half-space can be written as

$$E'(\mathbf{r},\omega_i) = -\frac{1}{4\pi}\int_{-\infty}^{+\infty}\mathrm{d}x' \left\{E'(x',\omega_i)[\frac{\partial G_0}{\partial z'} - D'(x')\frac{\partial G_0}{\partial x'}] - G_0 F(x',\omega_i)\right\}, \quad \mathbf{r}\in V'. \tag{8}$$

For numerical solutions to be implemented, the integral equation set of Eq. (6) can be numerically discretized into the following linear equation set[10,11]:

$$\begin{bmatrix} \mathbf{A}+\mathbf{I} & \mathbf{B} \\ \mathbf{A^{(0)}}-\mathbf{I} & \mathbf{B^{(0)}} \end{bmatrix}\begin{bmatrix} \mathbf{E} \\ \mathbf{F} \end{bmatrix} = 2\begin{bmatrix} \mathbf{E}^{(i)} \\ 0 \end{bmatrix}, \tag{9}$$

where $\mathbf{I}$ is the identity matrix, and the (m,n) elements of the $N\times N$ index matrices $\mathbf{A}$, $\mathbf{B}$ are given by

$$A_{mn} = \frac{i\sqrt{\varepsilon}k_0\Delta x}{2}\frac{D'(x_n)(x_m-x_n) - [D(x_m)-D(x_n)]}{\{(x_m-x_n)^2 + [D(x_m)-D(x_n)]^2\}^{1/2}} \times H_1^{(1)}(\sqrt{\varepsilon}k_0\{(x_m-x_n)^2 + [D(x_m)-D(x_n)]^2\}^{1/2}), \quad (m\neq n),$$

$$A_{mn} = \frac{-\Delta x}{2\pi\gamma^2}D''(x_n), \quad (m=n), \tag{10a}$$

$$B_{mn} = (i\Delta x/2)H_0^{(1)}(\sqrt{\varepsilon}k_0\{(x_m-x_n)^2 + [D(x_m)-D(x_n)]^2\}^{1/2}), \quad (m\neq n),$$

$$B_{mn} = (i\Delta x/2)H_0^{(1)}(\sqrt{\varepsilon}k_0\gamma\Delta x/2\mathrm{e}), \quad (m=n), \tag{10b}$$

where Δx is the step length. The elements for matrices $\mathbf{A^{(0)}}$ and $\mathbf{B^{(0)}}$ are also given by the above equations but

with the relative dielectric constant $\varepsilon = 1$ in vacuum instead of ε. The elements E_n and F_n of the vectors $\mathbf{E}$ and $\mathbf{F}$ are, respectively, the disretized electric field and its derivative. In the practical numerical performance, the numerical distributions of height $D(x)$ and the derivatives $D'(x)$ and $D''(x)$ are all zero. The number N of the sampling points is 1000 and that of frequency is 101. The refractive index $n = \sqrt{\varepsilon}$ of the medium is 1.532 for glass, and $\omega_0 = 2\pi\frac{c}{\lambda_0}(\lambda_0 = 800$ nm). The relation $H_\nu^{(1)}(Z) = J_\nu(Z) + iY_\nu(Z)$ is used, with J_ν is Bessel function and Y_ν Neumann function.

After the index matrices with the elements A_{mn}, B_{mn} and $A_{mn}^{(0)}$, $B_{mn}^{(0)}$ are constructed, the linear equation set is solved with the Gaussian elimination method[13], which gives the numerical distributions of $E(x,\omega_i)$ and its derivative $F(x,\omega_i)$ at the interface. The numerical distributions of transmitted light field $E'(\mathbf{r},\omega_i)$ at frequency ω_i are thereafter calculated based on Eq. (8).

The above calculation process is repeated for the light fields of all the frequency values of ω_i. In the frequency domain, discretization is made equidistantly with N_1 points and the step size $\Delta\omega_i = \Delta\omega_0/(N_1 - 1)$ in the range $[\omega_0 - \frac{\Delta\omega_0}{2}, \omega_0 + \frac{\Delta\omega_0}{2}]$, where size $\Delta\omega_0$ of the frequency range is so adjusted according to the width of the spectrum of the pulse that the contribution of component of the light wave outside this range can be neglected. The half-width of the spectrum is inversely proportional to τ, and so $\Delta\omega_0$ is adjusted in our calculation, N_1 is set to be 101.

With the spatial distributions of transmitted light field $E'(\mathbf{r},\omega)$ of all frequency values obtained, we can perform the digital inverse Fourier transform of $E'(\mathbf{r},\omega)$ with respect to ω at specific spatial point $\mathbf{r}$, from which the time-dependent light field $E'(\mathbf{r},t)$ at this point is obtained. Applying this transform to all the spatial points, we obtain the light field at any point $\mathbf{r}$ and at any time t. This enables us to understand either how the light field at a point $\mathbf{r}$ varies with time or how it behaves spatially at any moment. This is obviously important for the understanding of the construction and propagation of the light field of femtosecond pulse.

We calculate the light field distributions on the surface and transmitted in the vacuum half space with different half-widths of the laser pulses and different widths of the aperture. In Figs. 2(a) – (d) the transmitted light intensity distributions versus x are shown at the time instants which are symmetric with respect to the central time of the incident pulse and at the different distances from the interface. The width of laser pulse τ is 20 fs and size of the aperture is $L = 50$ nm. The time and the distance corresponding to each curve are given in the figures. We can see from the curves in each figure that before the central time $t = 0$ of the laser pulse, i.e., when $t < 0$, the light intensity of the central part is larger than that when $t > 0$, while the intensity away from the center, for $t < 0$ is smaller than that for $t > 0$. This is the apparent feature of the light intensity propagating along the direction parallel medium interface from the center of the aperture. Comparing the results of Figs. 2(b) and (d), we may see that in the near-field region, the larger is the distance from the medium interface, the larger is the intensity in the part away from the center of the aperture and the smaller in the part near the center for time $t > 0$.

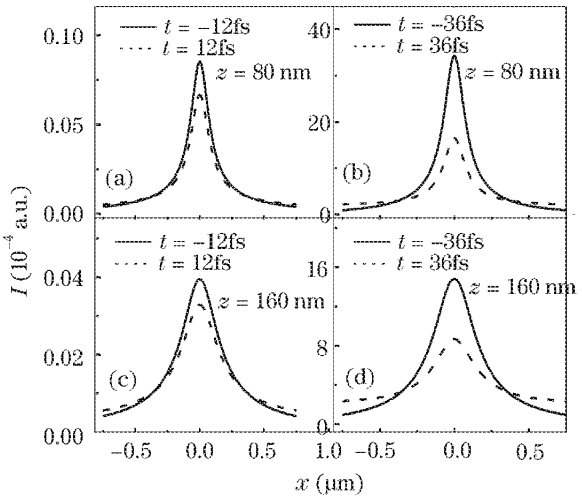

Fig. 2. The transmitted intensity distributions at the distance of 80 nm for (a) and (b), and 160 nm for (c) and (d). The width of the aperture is 50 nm. The pulse width is $\tau = 20$ fs.

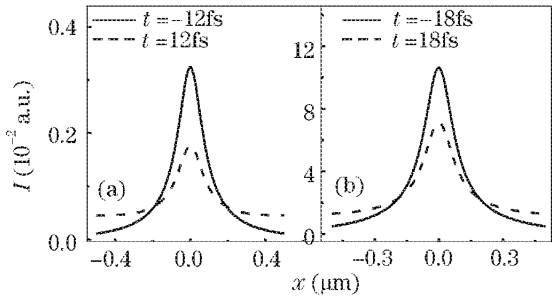

Fig. 3. The transmitted intensity distributions of a laser pulse with $\tau = 10$ fs at the distance of 80 nm and at time (a) $t = \pm 12$ fs and (b) $t = \pm 18$ fs.

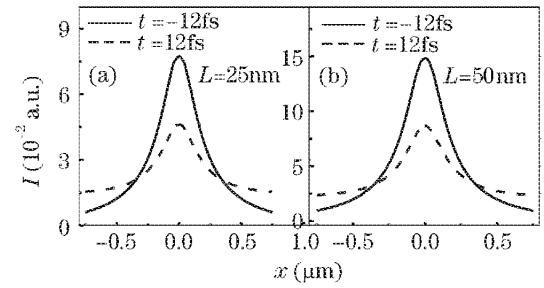

Fig. 4. The intensity curves of a laser pulse with $\tau = 20$ fs at the distance of 160 nm with the aperture sizes (a) 25 nm, (b) 50 nm and at time $t = \pm 12$ fs.

Figures 3(a) and (b) give the transmitted intensity distributions at the distance of 80 nm with $\tau = 10$ fs and at the time $t = \pm 12$ fs and $t = \pm 18$ fs, respectively. The size of the aperture is also 50 nm. We can see that the intensity distribution and the propagation feature of the light is about the same as that in Fig. 2.

Figures 4(a) and (b) show the intensity distributions at the distance of 160 nm for $\tau = 20$ fs with the aperture sizes 25 and 50 nm, respectively. The time for the curves in the figures are both $t = \pm 12$ fs. We may see

that though the absolute values of the intensity distribution is greater for larger aperture, the relative values in the parts away from the center of the aperture for smaller aperture are obviously larger. This is the evidence that smaller aperture excites relatively stronger evanescent waves that propagate in the direction along the medium interface and that is bound to the near-field of the interface.

To conclude, by using the solution of the Green's integral equation of electromagnetic waves at the medium boundaries, this paper proposes the method for the numerical calculation of the intensity distribution of the femtosecond laser pulse propagating through the subwavelength apertures. The preliminary results are obtained which shows how the light field propagates along the direction of the interface. We believe that the method and results are promising in the understanding of the process of the constructions and the propagations of the evanescent wave in area of the near-field optics.

X. Ren's e-mail address is renrxr@yahoo.com.cn, and C. Cheng's e-mail address is chengchuanfu@yahoo.com.

References

1. C. Girard and A. Dereux, Rep. Prog. Phys. **59,** 657 (1996).
2. J. J. Greffet and R. Carminati, Prog. Surf. Sci. **56,** 133 (1997).
3. R. C. Dunn, Chem. Rev. **99,** 2891 (1999).
4. M. Lefrancois and S. F. Pereira, Opt. Express **11,** 1114 (2003).
5. Z. Jiang, R. Jacquemin, and W. Eberhardt, Appl. Opt. **36,** 4358 (1997).
6. A. Pack, M. Hietschold, and R. Wannemacher, Ultramicroscopy **92,** 251 (2002).
7. R. Müller and C. Lienau, Appl. Phys. Lett. **76,** 3367 (2000).
8. A. Taflove, *Computational Electrodynamics* (Artech House, Norwood, 1995).
9. E. Vasilyeva and A. Taflove, Opt. Lett. **23,** 1155, (1998).
10. J. A. Sanchez-Gil and M. Nieto-Vesperinas, J. Opt. Soc. Am. A **8,** 1270 (1991).
11. A. A. Maradudin, T. Michel, A. R. Mcgurn, and E. R. Mendez, Ann. Phys. **203,** 255 (1990).
12. J. D. Jackson, *Classical Electrodynamics* (John Wiley & Sons, Inc., New York, London, Sydney, Toronto, 1975) p. 270.